

Validation and Updating of Industrial Models Based on the Constitutive Relation Error

D. Barthe*

EADS Launch Vehicles, 78130 Les Mureaux, France

and

A. Deraemaeker,[†] P. Ladevèze,[‡] and S. Le Loch[§]

Ecole Normale Supérieure de Cachan/Université Paris 6, 94235 Cachan Cedex, France

The validation and updating of models of industrial structures based on the concept of constitutive relation error is treated. The method is extended to the problem of the detection of defective sensors. The capabilities of the method are illustrated on the structure of the SYLDA5 double launching system of the European space launcher Ariane 5. The results obtained are encouraging and demonstrate the efficiency of the method for updating models of industrial structures.

Nomenclature

e_ω	=	modified constitutive relation error
$[G_r]$	=	norm matrix of the error on the measurements
H	=	Hooke's operator
$[K]$	=	stiffness matrix
k	=	structural parameters
$[M]$	=	mass matrix
$[T]$	=	reduced basis
U	=	displacements
\tilde{U}_ω	=	measured displacements at the sensors
V	=	displacements associated to σ
W	=	displacements associated to Γ
z	=	weighting factor
Γ	=	acceleration forces
ε	=	strain tensor
$\xi_{E\omega}$	=	relative constitutive relation error for each substructure
ξ_{sens}	=	sensors error contributions
ξ_ω	=	constitutive relation error
$\xi_{\omega r}$	=	relative constitutive relation error
ξ_0	=	required quality level
Π	=	projection operator
ρ	=	density
σ	=	stress tensor
ω	=	measured eigenfrequency

Introduction

THE importance of numerical simulations in industrial applications is constantly growing. Nevertheless, testing is still often found to be necessary because of the complexity of the structures. Thus, a small set of experiments is usually performed to validate the numerical model. Often, the correlation between tests and calculations is found to be rather poor. The discrepancies come mostly from the difficulty of modeling certain parts of the structure, for example,

joints or elements made of new materials such as composites, whose behavior is generally not well known.

When the predictions of the numerical model do not match the experimental results properly, model updating methods are used to minimize the distance between tests and calculations by acting on the numerical model. A state-of-the-art review of these methods may be found in Ref. 1. In the first category of methods, called direct methods, one seeks to correct the stiffness and mass matrices of the model without assigning any physical meaning to the modifications. In this category, one finds methods based on minimum norm corrections^{2,3} and methods based on control theory.^{4,5} Because the corrections are generally not physical, the validity of the corrected models is very limited when configurations other than the ones used for testing and updating are being considered.

The second category of methods is called indirect or parametric methods. In these methods, the corrections to the mass and stiffness matrices are based on physical parameters of the model. The approach consists of building a functional, which is usually called the cost function. This cost function represents the distance between the numerical model and the test data and is a function of the physical parameters of the model. Different types of cost functions can be used. We distinguish three categories: the input residual,^{6,7} the output residual,^{8,9} and the constitutive relation error (CRE). One major drawback of the first two categories is that the corresponding methods do not provide a measure of the quality of the updated model. This quality measure, however, is essential for model validation. The model updating method based on the CRE gives a quantitative measure of the correlation between the updated model and the test data and, thus, can be used for model validation. Its early developments date from the 1980s (Ref. 10). In a first stage, the method was developed for structural dynamics to update models based on eigenmodes and eigenfrequencies.¹¹ Later, the method was extended to deal with forced vibrations in Refs. 12 and 13. This approach uses the concept of Drucker error, and it has been found capable of dealing with the updating of mass, stiffness, and damping (see Ref. 14). It can also take into account nonlinearities due to the materials, as well as the effects of contacts. In another approach, presented in Ref. 15, the concept of dissipation error was applied to model updating. This error has a strong mechanical meaning and emphasizes the dissipation phenomena in the structure. The most recent applications of CRE-based model updating methods may be found in Refs. 15 and 16. There are also similar methods, such as minimum dynamic residual expansion¹⁷ or modeling error in the constitutive equations,¹⁸ applied to free vibrations.

Most of the methods mentioned give good results when applied to cases in which the amount of experimental data is significant compared to the complexity of the structure. This is often not the case with industrial structures. In addition, the numerical models used for

Received 29 March 2002; revision received 9 January 2003; accepted for publication 19 December 2003. Copyright © 2004 by the authors. Published by the American Institute of Aeronautics and Astronautics, Inc., with permission. Copies of this paper may be made for personal or internal use, on condition that the copier pay the \$10.00 per-copy fee to the Copyright Clearance Center, Inc., 222 Rosewood Drive, Danvers, MA 01923; include the code 0001-1452/04 \$10.00 in correspondence with the CCC.

*Director, Launchers Mechanical Analysis, 59 route Verneuil.

[†]Research Assistant, Laboratoire de Mécanique et Technologie—Cachan, Centre National de la Recherche Scientifique, 61 Avenue du Président Wilson.

[‡]Director, Laboratoire de Mécanique et Technologie—Cachan, Centre National de la Recherche Scientifique, 61 Avenue du Président Wilson.

[§]Ph.D. Student, Laboratoire de Mécanique et Technologie—Cachan, Centre National de la Recherche Scientifique, 61 Avenue du Président Wilson.

model updating have a large number of degrees of freedom, which makes the calculations very costly, and the constitutive relations can be quite complex, for composite materials, for example. All of these difficulties require the use of a robust updating method.

In this paper, we apply the CRE-based model updating method to an industrial structure. The method is based on the separation of the equations and quantities defining the problem into a reliable part and a less reliable part. For the numerical model, the constitutive relations are considered to be the less reliable equations. This leads to the construction of the CRE. This error can be calculated locally in a structure, and it allows one to determine in which regions of the model the constitutive relations are the most erroneous. Regarding the measurements, the measured amplitudes (force and displacement) are considered to be less reliable and lead to the construction of an error measure. Similarly, this error can be divided into contributions from each measurement (each sensor). In this paper, we show how this term can be used as an indicator of defective sensors (gain error, cabling error, etc.). Erroneous measurements can then either be corrected if the source of the error is found, or be removed. The cost function is the sum of the CRE and the errors on the measurements and is called the modified CRE. Once the measurements have been corrected, model updating can be carried out. The model updating method is iterative. Each iteration is divided into two steps. The first step consists in localizing the most erroneous regions in the structure based on the local value of the CRE. The second step consists in minimizing the modified CRE by acting only on the parameters that correspond to the regions selected in the previous step. After each iteration, the quality of the model is evaluated, and the model is validated when the error falls below a prescribed value.

In this paper, first, the CRE-based model updating method is reviewed in the case of linear structures based on eigenmodes and eigenfrequencies. Then, the method is extended to detect defective sensors from test data. An illustrative example is given for a beam model.

Then the model updating method is applied to an industrial structure. The structure is a double launching system of the European space launcher Ariane 5, called SYLDA5, which is capable of placing two satellites into their orbit. The finite element model has 28,000 degrees of freedom (DOF), and the structure is equipped with 260 sensors. The amount of experimental data is considerable but still small in relation to the complexity of the structure. The updating method allows one first to detect the defective sensors. Once these have been eliminated, model updating is carried out. Very good correlation is observed between the updated model and the test data.

Presentation of the Updating Method

Reference Problem

We consider a structure within a domain Ω during a time interval $[0, T]$ (Fig. 1). On the boundary $\partial\Omega$, displacements \mathbf{U}_d and forces \mathbf{F}_d are prescribed on $\partial_1\Omega$ and $\partial_2\Omega$, respectively. Body forces \mathbf{f}_d exist inside the domain Ω . The reference problem consists in finding the displacements $\mathbf{U}(\mathbf{M}, t)$, stresses $\boldsymbol{\sigma}(\mathbf{M}, t)$, and forces $\boldsymbol{\Gamma}(\mathbf{M}, t)$, $t \in [0, T]$, $\mathbf{M} \in \Omega$ that verify a set of equations that we subdivide into a reliable group and a less reliable group: The equilibrium equations are the reliable equations, and the constitutive relations are the less reliable equations.

To take into account both the free- and the forced-vibration cases, we will work in the frequency domain. In addition to the preceding equations, we need some data to solve the problem (frequency, direction and amplitude of the excitation, boundary conditions, etc.). In the framework of model updating, these data come from measurements on a real structure. For example, let us consider the case of the

free vibrations of a structure (eigenmodes and eigenfrequencies). In this case, we divide the data as follows: The reliable measurements are the measured eigenfrequency ω and the positions and directions of the sensors. The less reliable measurements are the amplitudes of the displacements at the sensors $\tilde{\mathbf{U}}_\omega$, which constitute a vector containing all of the measured values. This separation can vary depending on the problem and is given only as an example. The reliable quantities and equations define the admissible solution. We seek a solution that is admissible and that verifies the less reliable equations and quantities as closely as possible. The problem we must solve is

$$\begin{aligned} &\text{find } s \in S_{ad}^\omega \text{ that} \\ &P_\omega = \text{minimizes } e_\omega^2(s') \text{ with } s' \in S_{ad}^\omega \end{aligned} \quad (1)$$

where $e_\omega^2(s')$ is the modified CRE. In the case of free vibrations, the modified error at a given frequency is

$$e_\omega^2(s) = \xi_\omega^2(s) + [r/(1-r)] \|\Pi U - \tilde{\mathbf{U}}_\omega\|^2 \quad (2)$$

where $\xi_\omega^2(s)$ is the constitutive relation error and the second term represents the error on the measurements. Here $e_\omega^2(s)$ contains all of the less reliable quantities and equations that are to be verified by the admissible solution as closely as possible. Π is a projection operator, which when applied to the vector U gives the value of the vector at the sensors. In Eq. (2), $\|\cdot\|$ is an energy measure of error equivalent to $\xi_\omega^2(s)$. The coefficient $r/(1-r)$ is a weighting factor, which allows us to assign a greater or lesser degree of confidence to the measurements: The value of r is close to 1 if the measurements are considered very reliable and close to 0 in the opposite case. The value currently used is 0.5.

In the case of forced vibrations and multiple excitations, additional terms appear in the expression of $e_\omega^2(s)$ to take into account that the amplitudes of the measured forces are not reliable quantities. For more details, see Ref. 19.

The solution to this problem provides mechanical quantities $(\mathbf{U}, \boldsymbol{\sigma}, \boldsymbol{\Gamma})$ that satisfy exactly reliable equations, such as equilibrium, but do not satisfy less reliable quantities, such as the constitutive relations. This allows a residual to be built, which has a strong mechanical sense, based on the separation of the quantities and equations into reliable and less reliable ones. This residual is used to assess the quality of the model with respect to an experimental reference in which all of the data are not considered as reliable.

Modified Constitutive Relation Error

We consider the following constitutive relations:

$$\boldsymbol{\sigma} = \mathbf{H}\boldsymbol{\varepsilon} \quad (3)$$

$$\boldsymbol{\Gamma} = -\rho\omega^2\mathbf{U} \quad (4)$$

where ρ is the density (assumed to be constant). From these two constitutive relations, it is possible to build the CRE, which, for a given frequency (displacement formulation), is expressed as

$$\begin{aligned} \xi_\omega^2(\mathbf{U}, \mathbf{V}, \mathbf{W}) = &\int_\Omega \frac{\gamma}{2} \text{tr}\{\mathbf{H}[\boldsymbol{\varepsilon}(\mathbf{V}) - \boldsymbol{\varepsilon}(\mathbf{U})]^*[\boldsymbol{\varepsilon}(\mathbf{V}) - \boldsymbol{\varepsilon}(\mathbf{U})]\} \\ &+ \frac{1-\gamma}{2} \rho\omega^2(\mathbf{U} - \mathbf{W})^*(\mathbf{U} - \mathbf{W}) d\Omega \end{aligned} \quad (5)$$

where the asterisk represents the complex conjugate. We introduce fields \mathbf{U} , \mathbf{V} , and \mathbf{W} such that

$$\mathbf{U} = \mathbf{U} \quad (6)$$

$$\boldsymbol{\sigma} = \mathbf{H}\boldsymbol{\varepsilon}(\mathbf{V}) \quad (7)$$

$$\boldsymbol{\Gamma} = -\rho\omega^2\mathbf{W} \quad (8)$$

Fields \mathbf{V} and \mathbf{W} are fictitious fields representing $\boldsymbol{\sigma}$ and $\boldsymbol{\Gamma}$, respectively, to have a displacement formulation of the error that allows the problem to be discretized using the classical finite element method.

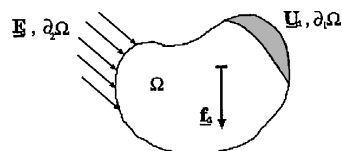


Fig. 1 Domain studied and applied loads.

Three fields are necessary because these quantities do not satisfy the constitutive relations and are, thus, supposed to be independent.

We also define the relative error

$$\xi_{\omega r}^2 = \xi_{\omega}^2 / D_{\omega}^2 \quad (9)$$

with

$$D_{\omega}^2 = \int_{\Omega} \frac{\gamma}{2} \text{tr}[(\mathbf{H})\varepsilon(\mathbf{U})^* \varepsilon(\mathbf{U})] + \frac{1-\gamma}{2} \rho \omega^2 \mathbf{U}^* \mathbf{U} \, d\Omega \quad (10)$$

When it is assumed that the structure is divided into substructures $E \in \mathbf{E}$, the error can be viewed as the sum of the contributions of all substructures

$$\xi_{\omega r}^2(s) = \sum_{E \in \Omega} \xi_{E\omega}^2(s) \quad (11)$$

The relative error for each substructure is given by

$$\begin{aligned} \xi_{E\omega}^2 = & \frac{1}{D_{\omega}^2} \int_E \frac{\gamma}{2} \text{tr}[\mathbf{H}[\varepsilon(\mathbf{V}) - \varepsilon(\mathbf{U})]^* [\varepsilon(\mathbf{V}) - \varepsilon(\mathbf{U})]] \\ & + \frac{1-\gamma}{2} \rho \omega^2 (\mathbf{U} - \mathbf{W})^* (\mathbf{U} - \mathbf{W}) \, dE \end{aligned} \quad (12)$$

When the structure is studied in a frequency range, we introduce a weighting factor $z(\omega)$ such that

$$\int_{\omega_{\min}}^{\omega_{\max}} z(\omega) \, d\omega = 1, \quad z(\omega) \geq 0 \quad (13)$$

The CRE in a frequency range is given by

$$\xi_T^2 = \int_{\omega_{\min}}^{\omega_{\max}} \xi_{\omega r}^2 z(\omega) \, d\omega \quad (14)$$

and the local contributions become

$$\xi_{ET}^2 = \int_{\omega_{\min}}^{\omega_{\max}} \xi_{E\omega}^2 z(\omega) \, d\omega \quad (15)$$

The modified CRE is now

$$e_T^2 = \int_{\omega_{\min}}^{\omega_{\max}} \frac{1}{D_{\omega}^2} e_{\omega}^2 z(\omega) \, d\omega \quad (16)$$

If the data consist of N eigenmodes and N eigenfrequencies, the function $z(\omega)$ is equal to $1/N$ at each of the eigenfrequencies and zero everywhere else. This function can be adjusted depending on the regions of interest in the frequency range. The value of ξ_T^2 represents the relative quality of the numerical model (in percent) with respect to the measurements.

Implementation of the Updating Method

Localization Step

For each experimental frequency ω , we solve the problem P_{ω} given by Eq. (1). The solution to this problem allows us to calculate the indicators ξ_T^2 , ξ_{ET}^2 , and e_T^2 . The value of ξ_T^2 represents the relative quality (in percent) of the numerical model with respect to the measurements in a certain frequency range. This allows us to decide whether model updating is necessary.

If model updating is considered necessary, we start from our mathematical model, which depends on a number of uncertain parameters, such as Young's modulus or the thickness of certain parts. We arrange these structural parameters into a vector \mathbf{k} ; we call the corresponding space $\langle \mathbf{k} \rangle$. The selection of the most erroneous substructures is based on the criterion

$$\xi_{ET}^2 \geq \delta \cdot \text{maximum}_{E \in \mathbf{E}} \xi_{ET}^2 \quad (17)$$

with, for example, $\delta = 0.8$. Note that large errors in all substructures indicate that the error distribution is nearly uniform in the structure. Let \mathbf{Z} be the set of the substructures that verify Eq. (17).

Correction Step

The localization step allows us to select the regions of the structure where the modeling error is large. Only parameters belonging to these substructures are selected for correction. The problem is to find $\mathbf{k} \in \langle \mathbf{k} \rangle_{\mathbf{Z}}$ that minimizes

$$\mathbf{k} \rightarrow J(\mathbf{k}) \quad (18)$$

$$\langle \mathbf{k} \rangle_{\mathbf{Z}} \rightarrow R \quad (19)$$

The functional $J(\mathbf{k})$ is defined by

$$J(\mathbf{k}) = \int_{\omega_{\min}}^{\omega_{\max}} \frac{1}{D_{\omega}^2} e_{\omega}^2 z(\omega) \, d\omega$$

This is a nonlinear problem with respect to the parameters in \mathbf{k} . We solve it using a Broyden–Fletcher–Goldfarb–Shanno (BFGS)-based minimization algorithm. The gradients of the cost function are calculated numerically. Thus, the stiffness and mass matrices are reassembled and problem P_{ω} is solved for each variation of the parameters.

Interruption of the Model Updating Process

Once the correction has been made, the value of ξ_T^2 is reevaluated. If it falls below the required quality level ξ_0^2 , the updating process is terminated and the model is considered valid. If not, a new iteration consisting of a localization and a correction step is performed. In each iteration, new erroneous substructures can appear as a result of the substructures from the previous stages being corrected. This approach provides a regularization of the inverse (ill-posed) problem.

Detection of Defective Sensors

Often, in practical cases where experimental data are available, some of the sensors give erroneous information. These defective sensors can have a negative influence on the localization process. We propose to use the modified CRE as a tool to detect potentially defective sensors before carrying out the updating of a structure.

The contribution of each sensor to the second term of the modified CRE is

$$\xi_{\text{sens}_\omega}^2 = \|\{\Pi \mathbf{U} - \tilde{\mathbf{U}}_{\omega}\}_{\text{sens}}\|^2 / D_{\omega}^2 \quad (20)$$

where $\{\cdot\}_{\text{sens}}$ is nonzero for sensor sens only. Here $\xi_{\text{sens}_T}^2$ is defined in the same way as ξ_{ET}^2 [Eq. (15)]. A large value of $\xi_{\text{sens}_T}^2$ compared to the values from the other sensors indicates that this sensor is defective. This can be easily understood from an engineering point of view. The solution of problem P_{ω} gives a displacement field \mathbf{U} whose general shape is imposed by the first term of the modified CRE. This solution is also required to match the experimental data as well as possible by the use of the second term of the error. If a sensor is defective, because the shape of the solution \mathbf{U} is given by the first term of the modified error, it will not be able to match the measurement at this point.

This explains why the detection of defective sensor is not very sensitive to small errors in the model: These do not affect the shape of \mathbf{U} as much as the defective sensor affects the measurements. This will be demonstrated on the beam example.

The measurements can then be corrected if the source of the error can be detected (sign or gain error). If such is not the case, the defective sensor is removed from the measurements. Then, the localization step is carried out once again with the corrected data.

Discrete Formulation and Reduction of the Size of Problem P_{ω}

The discretization of the problem using the finite element method leads to the construction of the stiffness and mass matrices \mathbf{K} and \mathbf{M} and the vectors of nodal values of the fields \mathbf{U} , \mathbf{V} and \mathbf{W} , which will be designated by $\{U\}$, $\{V\}$, and $\{W\}$.

Problem P_{ω} requires the linear system of equations to be solved:

$$[A]\{X\} = \{B\} \quad (21)$$

with

$$[A] = \begin{bmatrix} \gamma([K] - \omega^2[M]) & \frac{r}{1-r} \Pi^T [G_r] \Pi \\ -\left([K] + \frac{\gamma}{1-\gamma} \omega^2[M]\right) & ([K] - \omega^2[M]) \end{bmatrix} \quad (22)$$

$$\{X\} = \begin{bmatrix} \{U - V\} \\ \{U\} \end{bmatrix} \quad (23)$$

$$\{B\} = \begin{bmatrix} \frac{r}{1-r} \Pi^T [G_r] \{\tilde{U}_\omega\} \\ 0 \end{bmatrix} \quad (24)$$

Here, matrix $[G_r]$ represents the error measure $\|\cdot\|^2$. This problem is of large size. A reduction technique to overcome the high cost associated to the method is presented in Ref. 20.

Illustration: Beam Example

Presentation of the Problem

The approach we use for model updating is illustrated with the example of a beam that has both a model error and a defective sensor. This is a cantilever beam, and the part of the beam near the fixed end is five times less stiff than the rest. The beam is divided into 9 groups (180 DOF), with the stiffness defect in group 7 (Fig. 2).

The characteristics of the beam are 23 sensors; 1% measurement noise; +10% (stiffness) model error, group 7; and 50% error in defective sensor 10.

Initial Error and Detection of the Defective Sensor

The data consist of the first five modes. The localization step (Fig. 3) shows that the defective sensor (on group 4) impairs the determination of the localization of the stiffness error.

In the next step, we are attempting to find potential defective sensors. Therefore, we calculate the indicator $\xi_{sens_T}^2$ (Fig. 4).

This indicator clearly shows that sensor 10 is defective. Then, the localization step is carried out once again without taking this sensor into account, which enables us to localize the model error in group 7 (Fig. 5).

Correction Step

The parameters selected for correction are the stiffness and the mass of group 7. The minimization of $J(k)$ yields the results given in Table 1.

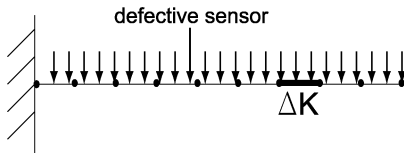


Fig. 2 Geometry, sensors, groups, and model error.

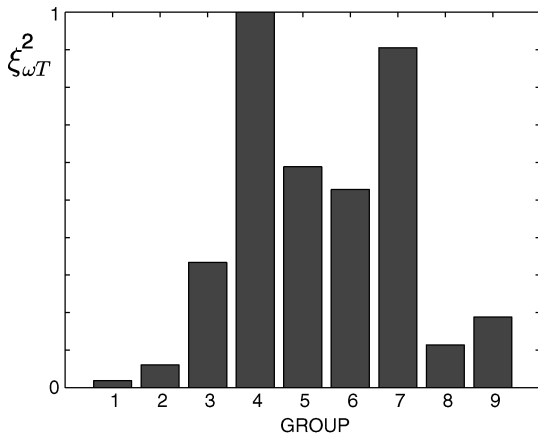


Fig. 3 Determination of the location of model errors.

Table 1 Minimization results

Group 7 parameter	Initial value	Correction	Corrected value	Reference value
E , Pa	390.5×10^9	1.1003	354.894×10^9	355×10^9
ρ , kg/m ³	2700	1.0061	2716.5	2700

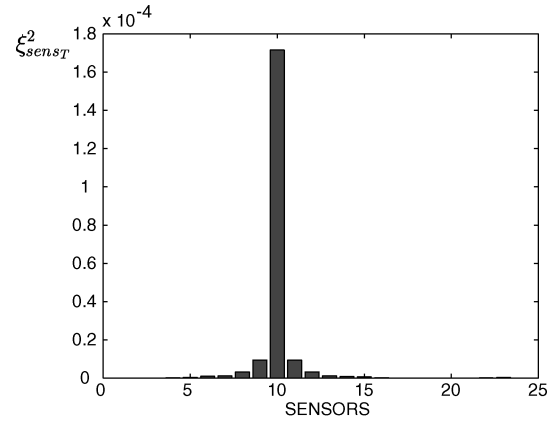


Fig. 4 The ξ_{sens}^2 indicator.

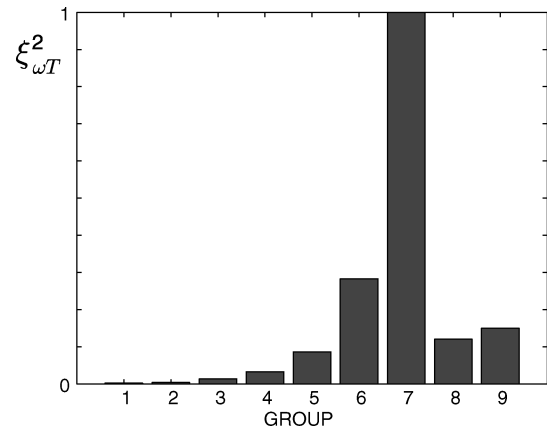


Fig. 5 Determination of the location of model errors.

This example illustrated the model updating method based on the CRE and showed that the proposed method is capable of detecting potentially defective sensors before the model updating step.

Remark on the Detection of Defective Sensors

It is interesting to see that the initial model error (stiffness error in group 7) has very little influence on the detection of the defective sensor. Let us consider the following example: 23 sensors; 1% measurement noise; +30% (stiffness) model error, group 7; and 2.5% error in defective sensor 10.

We plotted the value of $\xi_{sens_o}^2$ for each mode. Even though the defective sensor is not detected for each mode, the indicator $\xi_{sens_T}^2$ plotted in Fig. 6 allows us to detect the defective sensor clearly and is hardly influenced by the modeling error.

This can be easily understood because small model errors (compared to the dynamics of the whole system) do not affect the shape U very much compared to the distortion of the measurements caused by a defective sensor.

Updating of an Industrial Structure

Example: SYLDA5 Satellite Support

The updating method will be illustrated on an industrial model of a satellite support of the European launcher Ariane 5. This satellite support, called SYLDA5 (Fig. 7), allows the launcher to place two satellites into orbit.

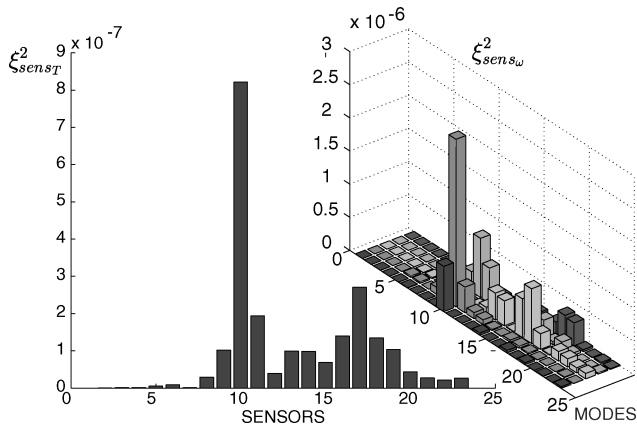


Fig. 6 Determination of the location of the defective sensor, contribution from each mode.

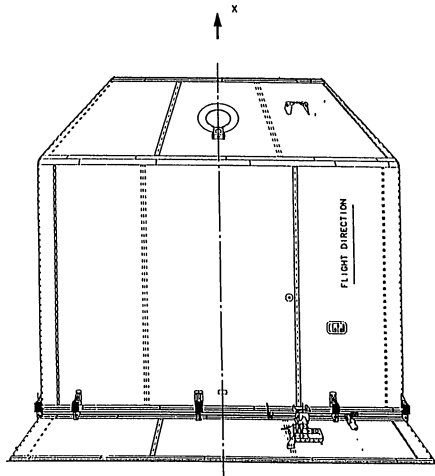


Fig. 7 SYLDA5 satellite support.

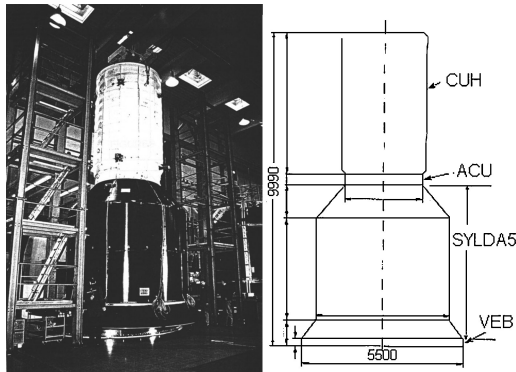


Fig. 8 Experimental setup.

Presentation of the Structure

To place SYLDA5 in a configuration similar to the one encountered in flight, the structure tested (Fig. 8) was composed of the following elements: 1) an upper payload dummy (CUH), which is a 3.5-ton ribbed steel cylinder with a 1.5-ton steel beam on top; 2) a payload adapter dummy (ACU), which is an aluminum ring; 3) SYLDA5, which is an assembly of cones and cylinders made of a sandwich composite (carbon/epoxy stratified layers, honeycomb aluminum core), with glued and bolted aluminum joints; and 4) ground binding system (VEB), which is an aluminum ring.

This structure is made of very different materials in terms of stiffness as well as density and has different types of joints. The geometry has rotational symmetry. Its total height is 10 m, and its diameter is 5 m.

Table 2 Characterization of the mode shapes

Mode N	Frequency, Hz	Mode shape
1, ..., 6	5–30	Bending, longitudinal, and torsion
7, ..., 12	40–100	Ovalization SYLDA/ACU

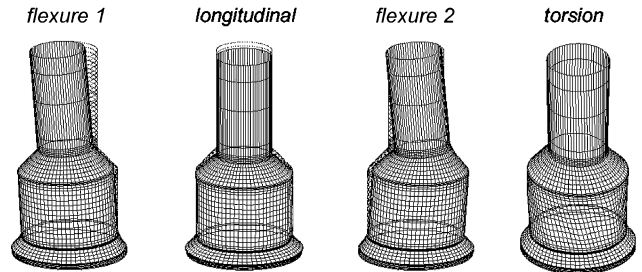


Fig. 9 First modes of the satellite support: 5–30 Hz.

Presentation of the Modal Tests

We used the results of the SYLDA5 industrial test campaign described in Ref. 21. The experimental modes were obtained by a force appropriation method using five exciters. A total of 260 accelerometers were placed in various parts of the structure.

Because of the symmetry, most of the modes are multiple modes. Because the frequencies are quite low, 5–100 Hz (Table 2), the eigenmodes consist of bending, traction, torsion, and radial expansion of the cylinders. The first modes of the satellite support are shown in Fig. 9.

The tests were not realized in specific dynamic testing facilities. As expected in this case for such structures, the ground to which the structure was attached underwent deformations. The contribution of the ground modified the modal results to some extent.

Finite Element Model

The model is made of plate elements for the cylinders and cones and beam elements for the joints and the upper beam of the CUH. The ribs of the CUH were not modeled: We used an orthotropic constitutive relation to model the stiffness variation in the different directions. The ground was represented by three rotational and three translational springs. The base of the structure was subjected to a prescribed rigid-body motion.

Because of the numerous joints and types of materials, the finite element model was divided into 30 different groups. Thus, if we limit the changes in each substructure to its mass and stiffness, the model is defined by 64 parameters. This shows the importance of the localization step to choose the parameters that have to be corrected. The localization process was performed by computing for each element the error that allows the stiffness or mass of one of the 9728 elements to be corrected.

The size of the finite element model was decreased by using a reduced basis; this lowered the number of DOF from 28,000 to 300. Note that the difficulties arising from multiple modes (double modes, mode pairing, etc.) do not affect the CRE updating method.

Initial Quality of the Model

The quality of the model is given by the total CRE. Its initial value was 12.39%. The classical indicators Δf and modal assurance criterion (MAC) and the CRE are shown in Table 3 for the 12 modes. These values indicate that modes 7 and 8 are very inaccurate (more than 30% error) and modes 11 and 12 are coupled CUH ovalization/SYLDA5 ovalization modes, which do not appear in the calculation of the eigenmodes (Fig. 10).

For the 10 other modes, the initial error is less than 10%.

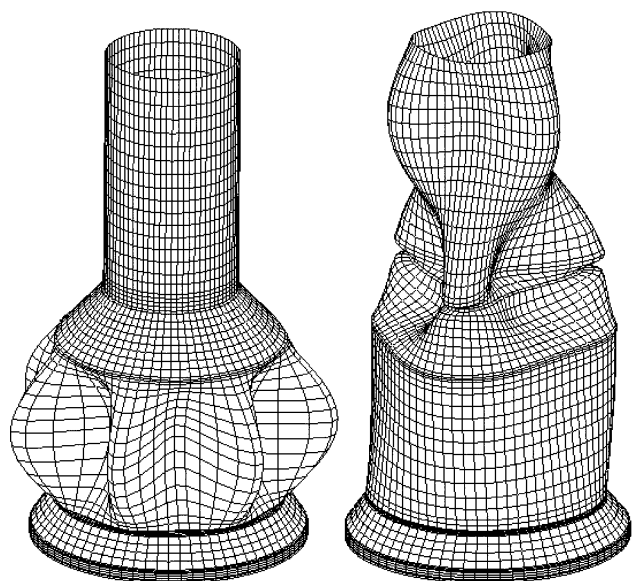
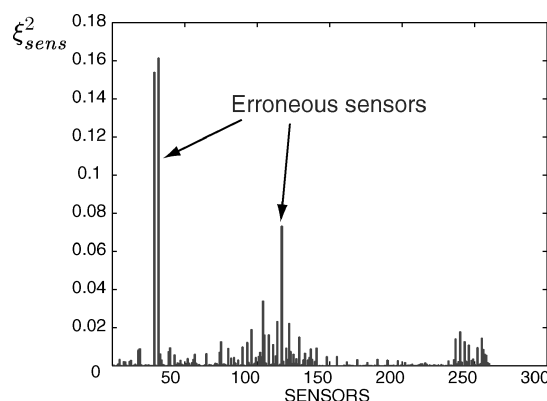
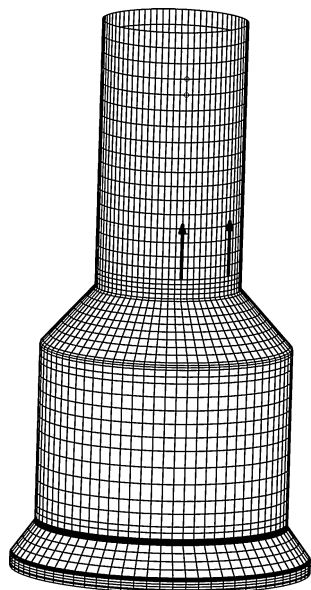
Detection of the Defective Sensors

During the appropriation of axial mode 3, defective sensors were detected. These sensors, located on the ACU, yielded accelerations that did not match the rigid-body motion of the payload for this mode (Fig. 11). Apart from easy cases such as this one, the detection of

Table 3 Discrepancy (percent error) in CRE and frequency during updating for all modes

Mode	Initial			Iteration 1		Iteration 2		Iteration 3		Iteration 4	
	ξ	Δf	MAC	ξ	Δf	ξ	Δf	ξ	Δf	ξ	Δf
1	3.45	-3.51	99.62	2.65	-2.69	0.24	0.28	2.05	2.05	1.67	1.86
2	3.25	-3.31	99.73	2.46	-2.49	0.39	0.37	2.19	2.15	1.54	1.43
3	5.10	-5.24	96.53	4.06	-4.14	0.40	-0.40	1.49	1.48	1.49	1.48
4	10.29	-10.85	99.11	9.78	-10.29	9.03	-9.48	4.09	-4.15	4.28	-4.22
5	9.86	-10.39	99.64	9.36	-9.83	8.61	-8.99	3.66	-3.75	3.76	-3.98
6	3.47	3.45 ^a	97.45	1.91	1.90 ^a	0.10	0.10 ^a	2.66	2.63	0.00	0.00
7	27.15	23.60	98.77	1.27	1.27	1.27	1.27	3.36	3.30	2.71	2.67
8	27.77	24.09	98.87	1.92	1.90	1.92	1.90	4.00	3.92	3.36	3.30
9	1.78	-1.79	96.14	0.09	-0.09	0.09	-0.09	0.02	0.02	0.10	-0.10
10	1.24	-1.24	95.84	0.44	0.44	0.44	0.44	0.55	0.55	0.43	0.43
11	6.41	*	*	1.01	*	1.04	*	2.11	*	1.65	*
12	4.82	*	*	0.64	*	0.63	*	1.36	*	0.56	*
ξ_T	12.39			4.32		3.69		2.62		2.27	

^aMode swapped with modes 4 and 5.

**Fig. 10** Calculated closed modes 21 and 22 ($\Delta f = 0.12$ Hz) corresponding to experimental mode 11.**Fig. 11** Defective sensors detected during the test.**Fig. 12** Detection of defective sensors.

defective sensors is not easy and usually requires the comparison of the MAC values with and without each sensor. (In addition, a rotation of the modes is necessary because of the symmetry of the problem, which makes the calculation of the MAC difficult.)

Let us illustrate our proposed method by using the $\xi_{sens_{no}}^2$ indicator on the example of the satellite support with the axial mode. This study was carried out separately for each mode because, inasmuch as appropriation was carried out independently for each mode, different defective sensors for each mode could be detected.

The detection process revealed the most defective sensors (Fig. 12), which were the same as the two identified during the test plus a third one whose defectiveness can be easily seen by comparing the experimental and numerical mode shapes. These three sensors were removed from the measurements before updating the structure. The same approach was carried out for the other modes.

Updating of the Structure

First Updating Stage: Localization Step

Figure 13 shows that the CRE is localized around the SYLDA5/ACU joint, on the plate part of the CUH and on the beam part of the CUH.

First Correction

The corrections to the parameters are given in Table 4. The numbers represent fractions of the initial values.

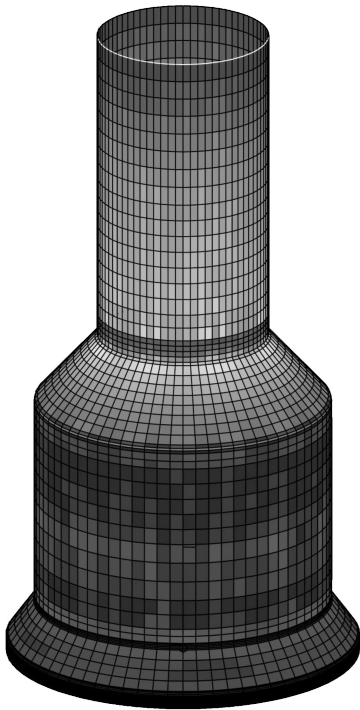
Corrected Regions

1) The initial coefficients of the CUH orthotropic plates chosen to represent the real CUH ribs were arbitrary; their modifications were expected.

2) The upper part of the CUH contains a simplified beam modeling; the error in this region was probably due to the influence of different ribs present on the real structure but was not modeled.

Table 4 Parameters selected and their corrected values after each iteration

Parameter	Iteration				
	0	1	2	3	4
<i>ACU joint</i>					
Beam	1	0		0.76	
E_1	1			0.57	
E_2	1			0.56	
G_{12}	1			1.79	
Lashing	1			0.09	
<i>Ground</i>					
T_x	1		0.25		
R_y	1		0.39		0.41
R_z	1		0.40		0.47
R_x	1		1.23		1.88
<i>CUH</i>					
Plates E_1	1	0.84			
Beam	1	6.36			6.51
ξ_T , %	12.39	4.32	3.69	2.62	2.27

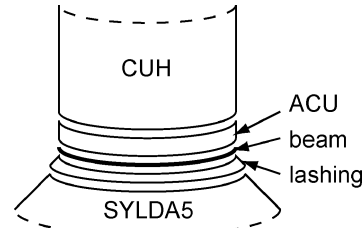
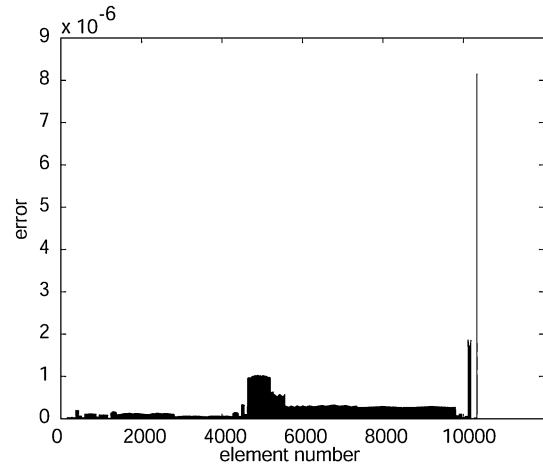
**Fig. 13** First localization step on SYLDA5.

3) Because the SYLDA5/ACU and ACU/CUH joints are very close (the height of the ACU substructure only 3% of the total height of the structure) and the SYLDA5/ACU is a rather complex joint, the ACU is not considered as a substructure but as a joint between the SYLDA5 and CUH. Therefore, it is modeled using a simplified model (orthotropic plates) aimed at representing correctly the behavior of the joint with equivalent stiffness parameters. The corrections on these parameters will thus not represent a modification of the real material stiffness modulus. The parameters of this region are presented Fig. 14.

Because the circular beam part is the most energetic part of this joint, it was the group detected with the most important error. The choice of other parameters of this region in a first iteration would not have been robust. The stiffness of the beam was corrected to zero, which means that the initial value was greatly overestimated.

Results of First Updating and Second Localization Step

The quality of the model went from 12.39 to 4.32% after the first correction. The model was much better, especially concerning modes 7 and 8 for which the error dropped from 27 to about 2% (Table 3). The new localization step showed the predominant error to be on the ground, which was expected because the initial stiffness

**Fig. 14** SYLDA5/ACU/CUH joint model.**Fig. 15** Second localization step.

values for the ground were just guesses. These errors are shown in Fig. 15, where the error is given for each element. (The ground is on the right-hand side.)

Subsequent Iterations

The following iterations are summarized in Table 4. The updating of the orthotropic parts of SYLDA5 was carried out separately for the longitudinal and transverse Young's moduli E_1 and E_2 . The process was also carried out separately for the membrane and the bending behavior of the plates. This enabled us to take into account the orthotropy of the material as well as the complex nature of the joints.

The updating of the ribbed cylinder CUH (modeled by an orthotropic cylinder) was carried out separately for the longitudinal and transverse Young's moduli E_1 and E_2 and for the shear modulus G . (Here, only E_1 was corrected.)

Analysis of Results After Updating

During iteration 3, the SYLDA5/ACU/CUH joint was corrected again. The beam stiffness and other parameters of this region were chosen because the total error is much lower than in the first iteration. After the correction, the beam stiffness regains a representative value and the lashing part becomes the part of the joint with a low stiffness (9% of the original).

The real joint is made of three parts in the SYLDA5: 1) an aluminum ring perpendicular to the launcher direction with the holes for the bolts, 2) an aluminum thin shell (a few millimeters thick), and 3) a connection between the composite sandwich of the body of the structure and the aluminum shell. This part is thick and a composite lashing with bolts is used to reinforce it.

The stiffness used for this joint (lashing in Fig. 14) was the estimated stiffness of the third part just listed. The correction found by the updating methods shows that the flexible aluminum shell has a great influence on this joint behavior and has to be taken into account.

Following the last correction, the error was localized only in the ground and the model could not be improved further. This shows that the model of the ground needs to be improved to get better results. However, one can see that the CRE is 2.27%, which is very small; therefore, the model can be considered valid.

Model updating allowed us to improve the model and to take into account the interaction with the ground. The SYLDA5/ACU/ CUH joint and the ground appeared to be the most critical regions to model.

Conclusions

In this paper, we extended the CRE model updating method to identify defective sensors from test data. This detection is based on the second term of the modified CRE, which is the error measure of the measurements.

The proposed approach was first illustrated on the simple example of a beam. It was then applied to the detection of defective sensors from test data of an industrial structure. This preliminary step allowed us to eliminate the most defective sensors before updating the structure. Then, we showed the efficiency of the proposed updating method. Only four iterations were needed to update the structure, and the updated model showed very good correlation with the test data. The low value of the CRE (2.27%) demonstrates the validity of the updated model.

Acknowledgments

This work is supported by the European Aeronautic Defence and Space Company Launch Vehicles Les Mureaux and the Centre National d'Etudes Spatiales (CNES) Evry. The SYLDA5 tests have been performed by Industrieanlagen-Betreibsgesellschaft for Daimler-Chrysler Aerospace/Dornier under a CNES (French Space Agency) contract.

References

- ¹Mottershead, J., and Friswell, M., "Model Updating in Structural Dynamics: A Survey," *Journal of Sound and Vibration*, Vol. 167, No. 2, 1993, pp. 347–375.
- ²Baruch, M., "Optimal Correction of Mass and Stiffness Matrices Using Measured Modes," *AIAA Journal*, Vol. 20, No. 11, 1982, pp. 1623–1626.
- ³Berman, A., and Nagy, E. J., "Improvement of a Large Analytical Model Using Test Data," *AIAA Journal*, Vol. 21, No. 8, 1983, pp. 1168–1173.
- ⁴Kaouk, M., and Zimmerman, D., "Structural Damage Assessment Using a Generalized Minimum Rank Perturbation," *AIAA Journal*, Vol. 32, No. 4, 1994, pp. 836–842.
- ⁵Zimmerman, D., and Kaouk, M., "Eigenstructure Assignment Approach for Structural Damage Detection," *AIAA Journal*, Vol. 30, No. 7, 1992, pp. 1848–1855.
- ⁶Berger, H., Ohayon, R., Quetin, L., Barthe, L., Ladèveze, P., and Reynier, M., "Méthodes de Recalage de Modèles de Structures en Dynamique," *La Recherche Aéronautique*, Vol. 5, 1991, pp. 9–20.
- ⁷Farhat, C., and Hemez, F., "Updating Finite Element Dynamic Models Using an Element-by-Element Sensitivity Methodology," *AIAA Journal*, Vol. 31, No. 9, 1993, pp. 1702–1711.
- ⁸Piranda, J., Lallement, G., and Cogan, S., "Parametric Correction of Finite Element Models by Minimization of an Output Residual: Improvement of the Sensivity Method," *Proceedings of IMAC IX*, Society for Experimental Mechanics, Bethel, CT, 1991, pp. 363–368.
- ⁹Lammens, S., Brughmans, M., Leuridan, J., Heylen, W., and Sas, P., "Application of a FRF Based Model Updating Technique for the Validation of a Finite Element Models of Components of the Automotive Industry," *Proceedings of Design Engineering Technical Conferences*, American Society of Mechanical Engineers, Fairfield, NJ, 1995, pp. 1191–1200.
- ¹⁰Ladèveze, P., "Updating of Complex Structures Models," *Aérospatiale*, TR 33.11.01.4, Les Mureaux, France, Oct. 1983.
- ¹¹Ladèveze, P., and Reynier, M., "A Localization Method of Stiffness Errors for the Adjustment of F. E. Models," *Vibrations Analysis Techniques and Applications, F.E. Modeling and Analysis*, Vol., American Society of Mechanical Engineers, Fairfield, NJ, 1989, pp. 355–361.
- ¹²Ladèveze, P., "Error on the Constitutive Relation in Dynamics: Theory and Application to Model Updating in Structural Dynamics," Lab. de Mécanique et Technologie, LMT Internal Rept. 150, Cachan, France, 1993.
- ¹³Ladèveze, P., Reynier, M., and Maia, N., "Error on the Constitutive Relation in Dynamics," *Inverse Problems in Engineering*, edited by H. D. Bui, M. Tanaka, et al., 1st ed., Balkema, Rotterdam, The Netherlands, 1994, pp. 251–256.
- ¹⁴Ladèveze, P., and Chouaki, A., "A Modelling Error Estimator For Dynamic Model Updating of Damped Structures," *Inverse Problems in Engineering Mechanics*, edited by M. Tanaka and G. S. Dulikravich, Vol. 1, Elsevier, Amsterdam, 1998, pp. 187–196.
- ¹⁵Chouaki, A., Deraemaeker, A., Ladèveze, P., and Le Loch, S., "Model Updating Using the Error in the Constitutive Relation : Real Case Study," *Proceedings of IMAC XVIII*, Society for Experimental Mechanics, Bethel, CT, 2000, pp. 140–146.
- ¹⁶Deraemaeker, A., Ladèveze, P., Collard, E., and Leconte, P., "Identification of Damped Joints Parameters Using the Error in the Constitutive Relation," *Inverse Problems in Engineering Mechanics*, edited by M. Tanaka and G. S. Dulikravich, Vol. 2, Elsevier, Amsterdam, 2000, pp. 367–376.
- ¹⁷Balmès, E., "Review and Evaluation of Shape Expansion Methods," *Proceedings of IMAC XVIII*, Society for Experimental Mechanics, Bethel, CT, 2000, pp. 555–561.
- ¹⁸Pascual, R., Golival, J., and Razeto, M., "On the Reliability of Error Localization Indicators," *Proceedings ISMA 23*, Katholieke Universiteit Leuven, Leuven, Belgium, 1998, pp. 1119–1127.
- ¹⁹Ladèveze, P., and Chouaki, A., "Application of A Posteriori Error Estimation for Structural Model Updating," *Inverse Problems*, Vol. 15, 1999, pp. 49–58.
- ²⁰Deraemaeker, A., Ladèveze, P., and Leconte, P., "Reduced Bases for Model Updating in Structural Dynamics Based on Constitutive Relation Error," *Computer Methods in Applied Mechanics and Engineering*, Vol. 191, No. 21–22, 2002, pp. 2427–2444.
- ²¹"A5-NT-1-X-2241-ASAI-Ed.1-Rev.1 06/05/99 Exploitation des Essais Dynamiques SYLDA5 et Validation du Modèle Dynamique Tridimensionnel ASAI du SYLDA5," EADs Launch Vehicles, Les Mureaux, France, 1999.

C. Pierre
Associate Editor